ISSN 1070-3632, Russian Journal of General Chemistry, 2014, Vol. 84, No. 3, pp. 424–432. © Pleiades Publishing, Ltd., 2014.
Original Russian Text © A.G. Kudrev, 2014, published in Zhurnal Obshchei Khimii, 2014, Vol. 84, No. 3, pp. 364–373.

Calculation of Equilibrium Formation Constants of Complexes with a Polydentate Oligomer

A. G. Kudrev

St. Petersburg State University, Universitetskii pr. 26, St. Petersburg, 198504 Russia
e-mail: kudrevandrei@mail.ru

Received November 18, 2013

Abstract—A methodology of the calculation of ligand−oligomer complex formation and cooperative binding constants by the matrix method is described. Theoretical analysis of the equilibrium binding between a ligand and a polydentate oligomer having a system of sites with different ligand affinities is performed. The simulated equilibrium complex formation between the oligonucleotide G4-DNA and porphyrin TMPyP4 was used to construct and analyze diagrams of the relative fraction of DNA−ligand complexes by the matrix method. Cooperative ligand binding to a system of nonequivalent sites can be established by chemometric analysis and rigid modeling of spectrophotometric titration data (in terms of the chemical equilibrium model).

DOI: 10.1134/S1070363214030037

Over the past years, much research interest has been focused on the structure and properties of multidentate oligomers containing conjugated sequences of guanine (G) bases forming, under certain conditions, 3D structures [1–4]. Such oligonucleotides were given the name G-quadruplexes (G4). Research into the mechanism of the DNA strand end to form a highly organized G4 structure (in the literature this structure is sometimes referred to as DNA tetraplex) [1], as well as into the mechanism of selective interaction of small probe molecules with such structures are associated with new anticancer drug development [5, 6]. Ligands are probes which exhibit a high affinity of G4 quadruplexes and are capable to induce DNA folding and inhibit telomerase in vivo [7–9]. The efficiency of a probe can be assessed by its affinity to G4 quadruplexes and selectivity. In the present work we consider ligand−oligomer interactions on an example simulating complex formation of G4 with the porphyrin TMPyP4 [5,10,15,20-tetrakis(1-methylpyridin-4-yl)porphyrin]. This porphyrin is widely used as a probe which allows one to detect G4 in solution in micromolar concentrations and to estimate the number of coordination vacancies in this important spacial DNA structure [4]. The advantage the TMPyP4 ligand offers for spectrometry consists in that the stoichiometry and stability of G4(TMPyP4)$_n$ complexes vary depending on the nucleotide structure of DNA.

$$\begin{gathered} \mathrm{G4 + TMPyP4 \rightleftarrows G4(TMPyP4)} \\ \ldots\ldots\ldots\ldots \\ \mathrm{G4(TMPyP4)_{n-1} + TMPyP4 \rightleftarrows G4(TMPyP4)_n.} \end{gathered} \quad (1)$$

Even though the equilibrium depends on the structure of G4, the character and parameters of the visible absorption spectra during TMPyP4 binding in water [reaction (1)] always vary in a similar way [10]. This fact allows us to simulate the matrix of spectra data by a preset equilibrium model, using the spectra of a free and a coordinated porphyrin. Mixing a solution of G-quadruplex with a solution of TMPyP4 at 25°C and pH 7 leads to a bathochromic shift (423±1 > 434±5 nm) and attenuation of the Soret band. These changes provide unequivocal evidence showing that the porphyrin forms one or several complexes with the general formula G4(TMPyP4)$_n$.

The aim of the present work was to describe the methodology and calculate the equilibrium constants of binding of the ligand with a multidentate ligand (with allowance for cooperative complex formation), using absorption spectrometry data.

The ligand−macromolecule binding was described in terms of the statistical or matrix approach, using a number of general equations [11–17]. The equations of complex formation in all the mentioned approaches are not based on experimental data. They only make it

possible to formulate a statistical theory which has to be verified. The hypothesis is accepted, if the deviation of theory from experiment in within an acceptable error level. In the present work we made use of the matrix method. This method was previously used to describe complex formation with mixed ligands [18–22], as well as to describe ligand binding with oligomers having both equivalent and nonequivalent sites [23–27]. The method is based on the assumption that binding of a ligand to one of the coordination vacancies of the central ion can affect the ligand affinity of the neighboring sites. This effect reveals itself in the cooperativity or antocooperativity of ligand−oligomer binding. The matrix method makes it possible to establish rules of the mutual effect of sites with account for their mutual arrangement (Fig. 1).

In the present work we applied the matrix method to a system of nonequivalent coordination vacancies. To find out whether the method is adequate enough or have certain limitations in the analysis of real experimental data, it should first be tested on simulated data.

Calculation of the equilibrium concentration of the ligand and the spectral forms of the oligomer. Let $Poly(L)_n$ complexes are formed under equilibrium conditions by the addition of the ligand (L) to a preset number of vacancies $n = 1, 2 \ldots N$ of the complex-forming agent (Poly). The entire set of complexes is present at any component concentrations, and the relative distribution of the oligomer between forms depends on the stability of the corresponding compounds. The entire set of $Poly(L)_n$ configurations is described by a configuration matrix $M(k,N)$ $k = 2^N - 1$. One matrix row M_k relates to one of the possible configurations of the complex: The sequences of zeroes relate to free sites and the sequences of units relate to ligand-occupied sites. Row-by-row multiplication of the configuration matrix by the intrinsic constants K (the binding constants of the ligand to individual sites in the absence of neighboring ligand-bound sites) and ω (interaction coefficients) gives the matrix M^* [Eq. (2)].

$$M\omega K = M^*. \quad (2)$$

The product of nonzero rows of the matrix M^* gives a column of microform stability $B(k,1)$ [Eq. (3)].

$$B = \prod_{j=1}^{N} (M^* - M + E). \quad (3)$$

Here E is the matrix of units of the same order as M.

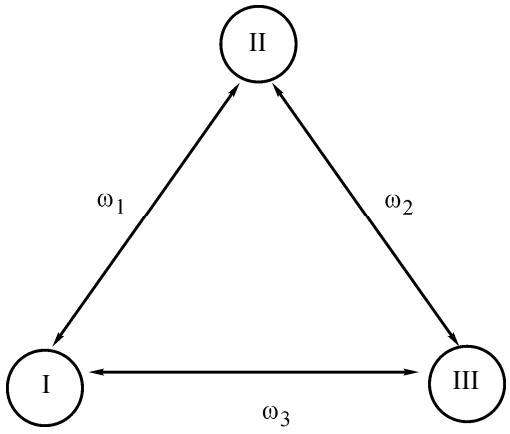

Fig. 1. Scheme of the suggested interaction between G-quadruplex sites.

At preset values of K_{1-N} and ω_i, the concentration of bound ligand is given by Eq. (4).

$$c_L - [L] = \frac{S[L]^S B}{1 + [L]^S B} c_P. \quad (4)$$

Here $S = \sum_{j=1}^{N} M^T$ is the row of stoichiometric coefficients; c_L and c_P, total concentration of the ligand and oligomer, respectively; and [L], equilibrium concentration of the ligand. Under the same conditions, the equilibrium concentration of complex forms of the oligomer can be calculated by Eq. (5).

$$[Poly(L)_S] = [Poly] \prod_{j=1}^{N} (M^*[L] - M + 1) = [Poly][L]^S B. \quad (5)$$

Here $[Poly] = c_P/(1 + [L]^S B)$ is the equilibrium concentration of free oligomer. Summing-up the corresponding microform concentrations, calculated by Eq. (5), gives Eq. (6) for the concentration of oligomer forms resulting from stepwise ligand binding.

$$c_{formPL}(i) = [Poly] \cdots \sum_{i=1}^{c_r^N} [Poly(L)_r] \cdots [Poly(L)_N]. \quad (6)$$

Here c_r^N is the number of possible variants of coordination r of ligands to an oligomer having N coordination vacancies, which is equal to the number of combinations from N by n. Equation (6) allows calculation of the matrix of equilibrium concentration of forms c_{formPL} at all ligand concentrations in the solution. The graphic representation of c_{formPL} is the diagram of oligomer distribution between complex forms as a function of the component concentrations in the solution.

Experiments revealed a spectral selectivity region in the intrinsic ligand adsorption range in the course of complex formation of G4-DNA with TMPyP4. Therefore, changes in the electronic absorption spectrum (EAS) can be correlated with changes in the concentrations of free and coordinated ligand.

The aim we set ourselves in using the matrix method was to calculate the intrinsic ligand binding model parameters K_{1-N} and ω_i. Depending on the method, the observed signal change can be associated with changes in the concentrations of different spectral forms. If signal change is associated with changes in the conformation or another property of the complex-forming molecule, the concentration matrix should contain the concentrations of microforms. In view of the great amount of microforms, one has to find the rank (R) of the summed concentration data matrix for microforms whose spectra best correlate with each other. The concentrations of spectral forms can be presented as the concentration matrix of free sites [Eq. (4)] and the concentration matrix of ligand-bound sites [Eq. (6)]. For each site j (j = 1, 2, …, N), the concentration of its bound ligand can be found by Eq. (7).

$$[\mathrm{Mon}_j\mathrm{L}] = [\mathrm{Poly(L)_S}]M. \quad (7)$$

Combining the calculated values, we obtain the concentration matrix of spectral forms c_f = {[L][$\mathrm{Mon_1L}$][$\mathrm{Mon_2L}$][$\mathrm{Mon_3L}$]}.

Calculation of target functions (data matrix). In the work we analyzed the possibility of calculations using two target functions. Let the first target function be the absorption matrix A_{exp}. According to the Lambert–Beer law, the spectrally measured absorption matrix A_{exp} can be decomposed into the concentration matrix of spectral forms c_f and the molar absorptivity matrix ε [Eq. (8)].

$$A_{exp} = c_f\varepsilon + \Delta. \quad (8)$$

Here Δ is the residual dispersion matrix (experimental noise matrix). The number of rows in the A_{exp} matrix is equal to the number of studied solutions with different component concentrations, and the number of columns in A_{exp} is equal to the number of wavelengths. In the analysis of real experimental data, the residual dispersion may also include systematic errors associated with unaccounted admixtures. This increases the theoretical rank of the matrix and makes the number of spectral forms difficult to estimate correctly. For a simpler and more illustrative analysis of simulated data, we omit from consideration both systematic and random errors. By multiplying both parts of Eq. (8) by the pseudo-inverse [28] matrix c_f^+ calculated with the initial estimates for the parameters to be refined, we obtain a current estimate for the real molar data matrix ε*.

$$\varepsilon^* = c_f^+ \cdot A_{exp}. \quad (9)$$

Here c_f^+ is the matrix pseudo-inverse [28] to the concentration matrix. To minimize the uncertainty of the mathematical solution, the iteration calculation is always subject to constraints. Both linear and nonlinear parameters for the chemical model were calculated with non-negativity constraints on concentrations and molar absorptivities. Multiplying ε* by c_f* gives A_{calc} for calculation of current values of the nonlinear parameters K_{1-N} and ω_i. Thus, the formula for calculation of the target function at current values of the target nonlinear parameters takes the following form:

$$A_{calc} = [c_f^+ \cdot A_{exp}]_{>0} \cdot c_f^*. \quad (10)$$

Here $[...]_{>0}$ is the operator which substitutes negative values by zeroes.

The second target function was that represented by the Job's plot. This function is calculated by Eqs. (11) and (12) with experimental data at any wavelength i in the region where the spectrum undergoes the most significant changes. This function corresponds to the theoretical function calculated by Eq. (13).

$$U = A_{exp} - c_L \cdot Sp\mathrm{L}, \quad (11)$$

$$J_{exp} = U_i/\max(U_i), \quad (12)$$

$$J_{calc} = (c_L - [\mathrm{L}])/\max(c_L - [\mathrm{L}]). \quad (13)$$

Molar absorptivity matrix. The molar absorptivity matrix was simulated using the Gaussian spectra calculated by Eq. (14).

$$E = \frac{\varepsilon^{-(X-\mu)^2/2\sigma^2}}{\sigma\sqrt{2\pi}}. \quad (14)$$

Here X is a selected sequence of numbers from 1 to 10. Parameters of Eq. (14) were chosen so that the simulated spectra reproduced the characteristic absorption spectra of the porphyrin TMPyP4 (SpL) and its complexes with the G4-DNA quadruplex (Sp1, Sp2). The calculated spectra were combined to form the molar absorptivity matrix ε = [SpL Sp1 Sp2 Sp1] whose graphic representation is shown in Fig. 2.

Simulated spectra are preferred for theoretical analysis, because in this case one does not need to include the hardly reproducible experimental noise.

For optimal parametrization of the matrix model we made use of the standard Levenberg−Marquardt nonlinear least-squares algorithm [29, 30] which is known to be efficient for calculation of equilibrium constants by spectrophotometric titration data. By varying independent variables we minimized the sum of squared deviations of all values of the target function F_{exp} from the corresponding values F_{calc} calculated at every iteration step by Eq. (15).

$$S = \Sigma(F_{exp} - F_{calc})^2. \quad (15)$$

The refinement procedure was terminated, when the difference between two successive iterations becomes smaller than the threshold value. According to the maximum likelihood principle and under the condition of uniform dispersion values, parameters corresponding to the minimum of the S function relate to the maximally likelihood model of the system.

Depending on the target function, the procedures for calculation of K_{1-N} and ω_i we denote *Sp*–LS and Job–LS. In the first case, $F_{exp} = A_{exp}$ and $F_{calc} = A_{calc}$ (*Sp*–LS); calculations are performed by Eqs. (7)–(10) and (14). In the second case, $F_{exp} = J_{exp}$ and $F_{calc} = J_{calc}$ (Job–LS); calculations are performed by Eqs. (11)–(14). The quality of fit of calculated to theoretical concentration profiles is assessed using the Hamilton factor [31, 32]. Expressing the Hamilton factor in percent and omitting the weight coefficients, we obtain a criterion which allows us to assess simultaneously the quality of fit of calculated to theoretical data for absolute concentrations and shapes of concentration profiles. The errors are calculated by Eq. (16).

$$\text{lof} = \frac{\text{Trace}[(F_{exp} - F_{calc})(F_{exp} - F_{calc})^T]}{\text{Trace}[F_{exp}F_{exp}^T]} \times 100\%. \quad (16)$$

Here (Trace) is the sum of diagonal matrix elements.

As mentioned above, it is suggested that G-quadruplexes have 3 coordination vacancies. Figure 1 depicts the possible interactions between sites of the complex-forming agent. Let us consider the case when all sites in G-4 are equivalent. In this case, ligand coordination to each site individually produces similar electron density redistributions, and, as a result, similar changes in the EAS of the ligand. At varied concentrations of the components (G4 and L) of the solution, the absorption dispersion in the intrinsic absorption range of the ligand will depend on two principal factors, which corresponds to rank 2 of the data matrix (Table 1). The experimental absorption data can be calculated by Eq. (17).

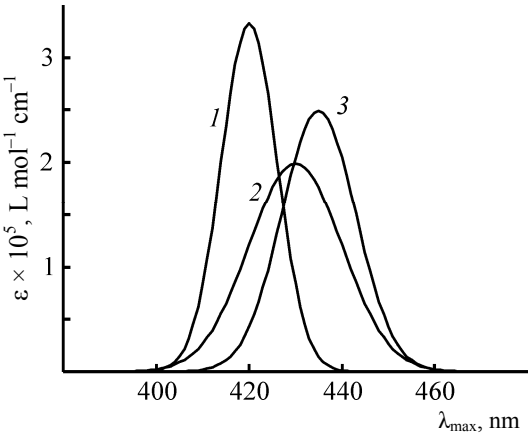

Fig. 2. Molar absorption spectra of the (*1*) free ligand (*Sp*L) and ligand coordinated to (*2*) sites I and III (*Sp*1), and (*3*) site II (*Sp*2).

$$A_{exp} = c_f[SpL\ Sp1\ Sp1\ Sp1] + \Delta. \quad (17)$$

Here *Sp*L is the EAS of free ligand; *Sp*1, EAS of the ligand coordinated to sites I–III. Figure 2 shows the *Sp*L and *Sp*1 spectra used to simulate A_{exp}. The normalized site concentration curves $f_c(RU) = [Mon_1L\ Mon_2L\ Mon_3L]/c_P$, calculated by Eq. (7) for the given case, are shown in Fig. 3a. The same figure shows the distribution of the G4 oligomer by the forms of complexes (c_{formPL}), calculated by Eq. (6). When G4 sites are equivalent, optimization by the Job–LS or *Sp*–LS procedure gives theoretical values of the binding model parameters K_{1-3} and ω_i. Simulation provides evidence showing that correct solution can be obtained by optimization in the space of one or two independent variables (parameters of the model) (Table 1).

An experimental example of the above-considered situation was described by Jaumot et al. [33], who concluded that the addition of TMPyP4 to a G4-quadruplex (krasG1) forms exclusively a 1 : 3 complex. This conclusion was drawn from the fact that the singular value decomposition (SVD) revealed three main spectral forms. These three forms were assigned to the oligonucleotide krasG1 form (whose spectrum has a characteristic maximum at 250 nm), free TMPyP4 (whose spectrum has a characteristic Soret band at λ_{max} 422 nm), and TMPyP4−krasG1 complex (λ_{max} 440 nm). As the concentration of krasG1 increased, the intensity of the Soret band decreased and the intensity of the band at 440 nm increased.

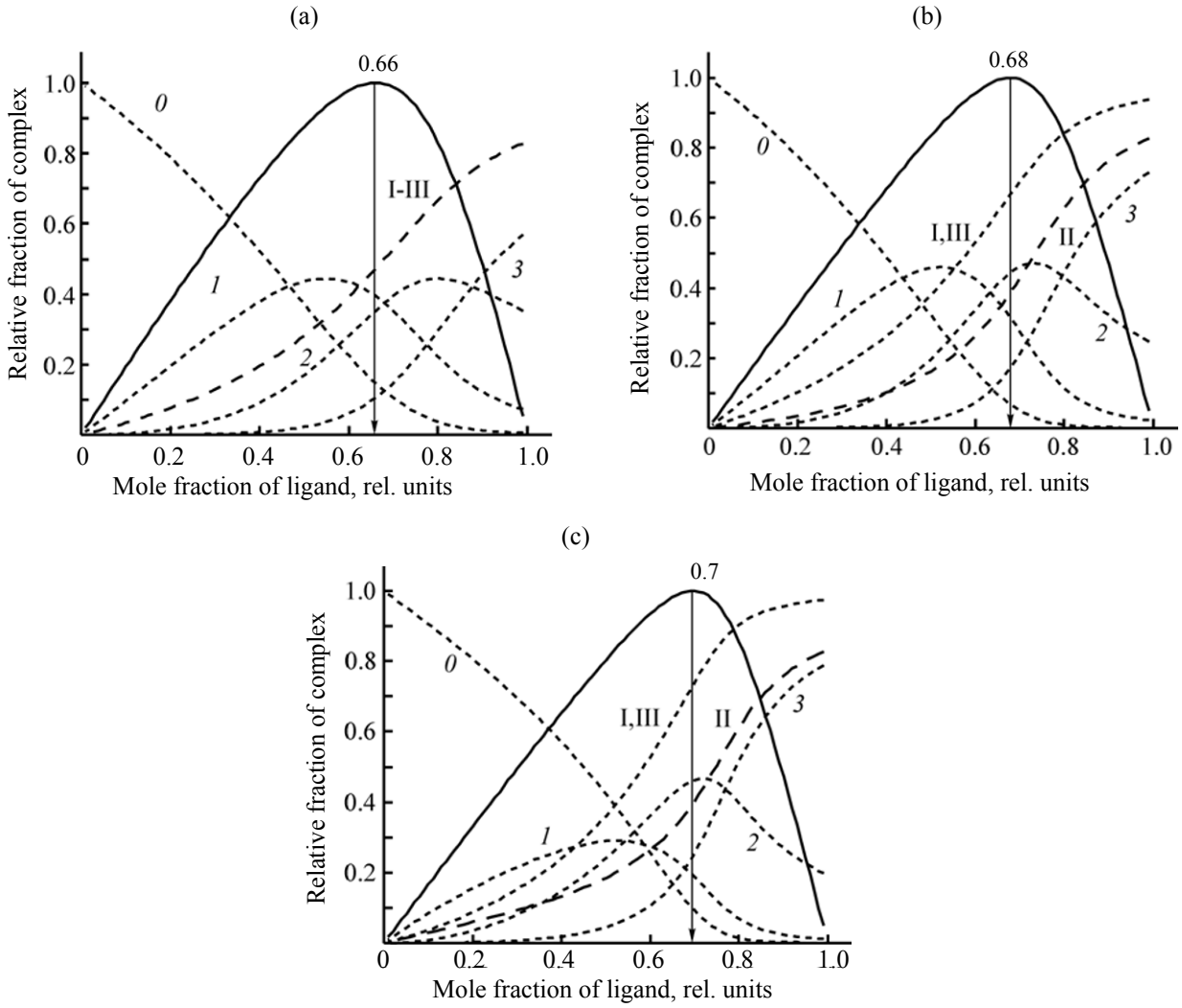

Fig. 3. Concentration dependences used for simulations. (a–c) Distributions of the complex-forming agent by the Poly(L)$_n$ complex forms (the curve numbers correspond to n) vs. mole fraction of the ligand RU [RU = = $c_L/(c_L + c_P)$; $c_L + c_P = 5$ μM]: (dashed lines) relative contents of sites (j = I, II, III) coordinated to the ligand, [$Mon_1LMon_2LMon_3L$]/c_P and (solid lines) Job's plots. The plots are calculated by the matrix method with the following binding parameters: (a) log $K_{1–3}$ = [6 6 6], $\omega_1 = \omega_2 = \omega_3 = 1$; (b) log $K_{1–3}$ = [6.5 6 6.5], $\omega_1 = \omega_2 = \omega_3 = 1$; and (c) log $K_{1–3}$ = [6 6 6], $\omega_1 = \omega_2 = 1$; $\omega_3 = 3$.

A different behavior of a G-quadruplex is observed, when one of the sites differ from the two others in ligand affinity. The rank of the matrix for this system depends on whether the EAS of the ligand undergoes similar or dissimilar changes on coordination. The normalized site concentration curves f_c(RU) = [Mon_1L Mon_2L Mon_3L]/c_P for this case are shown in Fig, 3b. Let us consider the case when coordination of the ligand leads to similar changes in its EAS spectrum, i.e. the A_{exp} matrix can be presented by Eq. (17). With parameters set for simulation, the matrix method gives correct solution of the inverse task irrespective of the optimization procedure (Job–LS or *Sp*–LS), provided optimization is performed in the space of two equilibrium constants (Table 1). Verification of the cooperativity hypothesis under the assumption of equal ligand affinities of sites show that the A_{exp}. matrix is reproduced with a very low error. In a real experiment, such error is unlikely to be differentiated from experimental noise. To overcome the experimental uncertainty, optimization should involve three independent variables. Simultaneous calculation of two equilibrium constants and cooperativity parameter leads to correct results (Table 1).

Table 1. Suggested models of ligand binding with sites I–III of G4, corresponding to Fig. 1 (without cooperativity, ω_i 1) and calculated by the LSM[a] procedure

Simulated model					LSM results			
site no.	log K_{1-3}	*Sp*Sim	Rank R_{MatSp}	f_{exp}–f_{calc}	calculated parameters	Job–LS log K_{Job}	r_{max}	*Sp*–LS log K_{Sp}
I II III	6 6 6	*Sp*L *Sp*1 *Sp*1 *Sp*1	2	0	$K_1 = x(1)$ $K_2 = x(2)$ $K_3 = x(1)$ $\omega_i = 1$[b]	6.0 6.0 6.0 (lof ≈ 0[c])	0.66	6.0 6.0 6.0 (lof ≈ 0)
					$K_1 = x(1)$ $K_2 = x(2)$ $K_3 = x(1)$ $\omega_i = 1$[b]	6.5 6.0 6.5 (lof ≈ 0)	0.68	6.5 6.0 6.5 (lof ≈ 0)
I II III	6.5 6 6.5	*Sp*L *Sp*1 *Sp*1 *Sp*1	2	0	$K_1 = x(1)$ $K_2 = x(1)$ $K_3 = x(1)$ $\omega_1 = \omega_2 = 1$[b] $\omega_3 = x(2)$	6.4 6.4 6.4 $\omega_3 = 0.8$ (lof = 4×10^{-3})	0.68	6.4 6.4 6.4 $\omega_3 = 0.8$ (lof = 2×10^{-3})
					$K_1 = x(1)$ $K_2 = x(2)$ $K_3 = x(1)$ $\omega_1 = \omega_2 = 1$[b] $\omega_3 = x(3)$	6.5 6.0 6.5 $\omega_3 = 1.0$ (lof ≈ 0)	0.68	6.5 6.0 6.5 $\omega_3 = 1.0$ (lof ≈ 0)
					$K_1 = x(1)$ $K_2 = x(2)$ $K_3 = x(1)$ $\omega_i = 1$[b]	6.4 6.4 6.4 (lof = 0.5)	0.68	6.5 6.0 6.5 (lof ≈ 0)
I II III	6.5 6 6.5	*Sp*L *Sp*1 *Sp*2 *Sp*1	3	*f*(RU)	$K_1 = x(1)$ $K_2 = x(1)$ $K_3 = x(1)$ $\omega_1 = \omega_2 = 1$[b] $\omega_3 = x(2)$	5.74 5.74 5.74 $\omega_3 = 4.0$ (lof = 0.2)	0.68	5.56 5.56 5.56 $\omega_3 = 6.8$ (lof = 0.4)
					$K_1 = x(1)$ $K_2 = x(2)$ $K_3 = x(1)$ $\omega_1 = \omega_2 = 1$[b] $\omega_3 = x(3)$	5.69 5.72 5.69 $\omega_3 = 4.4$ (lof = 0.2)	0.68	6.5 6.0 6.5 $\omega_3 = 1.0$ (lof ≈ 0)

[a] (LSM) Least-squares method. [b] Fixed parameter. [c] lof < $10^{-3} \approx 0$; $c_L + c_P = 5$ μM.

An experimental example of the system with different sites in a G4 oligomer can be found in the paper of Manaye et al. [34], who showed that the addition of TMPyP4 to G4 (ckit2) forms two complexes (1 : 1 and 1 : 3). The scheme of complex formation in the cited work was explained by the presence of two types of sites having different ligand affinities. The experimental absorption matrix is given be Eq. (18).

$$A_{exp} = c_f[SpL\ Sp1\ Sp2\ Sp1] + \Delta. \quad (18)$$

Here *Sp*L is the EAS of free ligand and *Sp*1 and *Sp*2, spectra of the ligand coordinated to sites I, III and II, respectively. According to Eq. (18), the absorption dispersion in the intrinsic absorption range of the ligand will depend on three principal factors, which corresponds to rank 3 of the data matrix.

If the rank of the data matrix is 3, then the J_{calc} function used in the optimization procedure Job–LS will differ from the J_{exp} function [Eq. (12)]. Consequently, the model parameters calculated by this procedure will differ from true parameters. Thus, the fact that the Job–LS and *Sp*–LS procedure give different parameters provides clear evidence showing that one of the sites differ from the other two sites.

Table 2. Suggested models of ligand binding with 3 equivalent coordination vacancies (cooperativity included) and parameters calculated by the LSM procedure

Simulated model					LSM results			
site no.	log K_{1-3}	*Sp*Sim	Rank $R_{Mat Sp}$	f_{exp}–f_{calc}	calculated parameters	Job–LS log K_{Job}	r_{max}	*Sp*–LS log K_{Sp}
I II III	6 6 6 $\omega_1 = \omega_2 = 1$ $\omega_3 = 3$	*Sp*L *Sp*1 *Sp*1 *Sp*1	2	0	$K_1 = x(1)$ $K_2 = x(2)$ $K_3 = x(1)$ $\omega_1 = \omega_2 = \omega_3 = 1$[a]	6.52 6.52 6.52 (lof = 0.4)	0.7	6.5 6.4 6.5 (lof = 0.1)
					$K_1 = x(1)$ $K_2 = x(2)$ $K_3 = x(1)$ $\omega_1 = \omega_2 = 1$[a] $\omega_3 = x(3)$	6 6 6 $\omega_3 = 3$ (lof ≈ 0[b])	0.7	6 6 6 $\omega_3 = 3$ (lof ≈ 0)
I II III	6 6 6 $\omega_1 = \omega_2 = 1$ $\omega_3 = 3$	*Sp*L *Sp*1 *Sp*2 *Sp*1	3	*f*(RU)	$K_1 = x(1)$ $K_2 = x(2)$ $K_3 = x(1)$ $\omega_1 = \omega_2 = \omega_3 = 1$[a]	6.51 6.51 6.51 (lof = 1.3)	0.7	6.57 6.19 6.57 (lof = 0.6)
					$K_1 = x(1)$ $K_2 = x(2)$ $K_3 = x(1)$ $\omega_1 = \omega_2 = 1$[a] $\omega_3 = x(3)$	6.0 6.4 6.0 $\omega_3 = 2.2$ (lof = 0.3)	0.7	6 6 6 $\omega_3 = 3$ (lof ≈ 0)

[a] Fixed parameter. [b] lof < 10^{-3} ≈ 0; $c_L + c_P = 5$ μM.

Table 3. Suggested models of ligand binding with nonequivalent sites I–III of G4, corresponding to Fig. 1 (cooperativity included), and parameters calculated by the LSM procedure

Simulated model					LSM results			
site no.	log K_{1-3}	*Sp*Sim	Rank $R_{Mat Sp}$	f_{exp}–f_{calc}	calculated parameters	Job–LS log K_{Job}	r_{max}	*Sp*–LS log K_{Sp}
I II III	6.5 6 6.5 $\omega_1 = \omega_2 = 1$ $\omega_3 = 3$	*Sp*L *Sp*1 *Sp*1 *Sp*1	2	0	$K_1 = x(1)$ $K_2 = x(2)$ $K_3 = x(1)$ $\omega_1 = \omega_2 = 1$[a] $\omega_3 = x(3)$	6.5 6 6.5 $\omega_3 = 3$ (lof ≈ 0[b])	0.7	6.5 6 6.5 $\omega_3 = 3$ (lof ≈ 0)
I II III	6.5 6 6.5 $\omega_1 = \omega_2 = 1$ $\omega_3 = 3$	*Sp*L *Sp*1 *Sp*2 *Sp*1	3	*f*(RU)	$K_1 = x(1)$ $K_2 = x(2)$ $K_3 = x(1)$ $\omega_1 = \omega_2 = 1$[a] $\omega_3 = x(3)$	5.4 6.2 5.4 $\omega_3 = 19$ (lof = 0.5)	0.7	6.5 6 6.5 $\omega_3 = 3$ (lof ≈ 0)

[a] Fixed parameter. [b] lof < 10^{-3} ≈ 0; $c_L + c_P = 5$ μM.

The energy effect of the addition of a further ligand in the course of the stepwise process, too, can be associated with the cooperativity effect. Let us consider the case of cooperative addition to a system of equivalent sites (Table 2). The normalized site concentration curves for this case are presented in Fig. 3c. The same figure shows the distribution of the G4 oligomer by the forms of complexes (c_{formPL}),

calculated by Eq. (6). Comparison of Figs. 2 and 3c shows that cooperativity shifts the λ_{max} in the Job's plot to aigher mole fractions of the ligand. Cooperativity results in that the initially equivalent sites behave as nonequivalent. This conclusion follows from a comparison of Figs. 3b and 3c.

If ligand coordination to each site individually produces similar changes in the extinction of free ligand, the experimental absorption matrix can be calculated by Eq. (17). The simulated A_{exp} matrix has rank 2. As seen from Table 2, optimization without inclusion of cooperativity gives different solutions depending on the optimization procedure (Job–LS or *Sp*–LS). The solution can be improved (to obtain a lower lof) by using the cooperativity parameter as an independent variable. In the latter case, the solution is independent on the optimization procedure (Job–LS or *Sp*–LS). The increase of the rank can be explained by that the cooperative binding affects the EAS of the reaction product. If the A_{exp} rank is equal to 3, evidence for cooperative binding can be provided by the fact that the solution resulting from the optimization the space of three independent variables is better than that with two independent variables. The best fit of calculation to experiment is obtained by the *Sp*–LS procedure.

Cooperativity of complex formation also reveals itself in the case of nonequivalent sites (Table 3). If the rank of the A_{exp} matrix is 2, both Job–LS or *Sp*–LS optimization provides theoretical values of the binding model parameters $K_{1–3}$ and ω_i. If the rank of the A_{exp} matrix is 3, the inclusion of three independent variables results is a better solution compared to that resulting from optimization in the space of two independent variables. The theoretical parameters of complex formation, that are a solution of the inverse task, can be obtained by the *Sp*–LS procedure (Table 3).

In conclusion we can note that cooperative ligand binding to an oligomer containing a system of three coordination sites can be revealed from spectrophotometry data by the matrix method with nonlinear least-squares optimization.

The most important criterion is the rank of the analyzed visible absorption matrix. The model is based on the model that accounts the mutual effect of ligands in stepwise complex formation with a system of coordination vacancies of the complex-forming agent. It was shown for the system simulating G4-DNA–porphyrin reaction that correct parameters of ligand addition can be calculated using the Job–LS or *Sp*–LS procedures described in the present work, provided the rank of the absorption matrix is 2. In cases where the rank of the experimental data matrix is 3, correct solution of the inverse task can be obtained by the *Sp*–LS procedure.

REFERENCES

1. Neidle, S. and Balasubramanian, S., *Quadruplex Nucleic Acids*, Cambridge: Roy. Soc. Chem., 2006.
2. Georgiades, S.N., Abd Karim, N.H., Suntharalingam, K., and Vilar, R., *Angew. Chem. Int. Ed*., 2010, vol. 49, p. 4020.
3. Murat, P., Singh, Y., and Defrancq, E., *Chem. Soc. Rev*., 2011, vol. 40, no. 11, p. 5293.
4. Largy, E., Granzhan, A., Hamon, F., Verga, D., and Teulade-Fichou, M.P., *Top. Curr. Chem*., 2013, vol. 330, p. 111.
5. Boncina, M., Lah, J., Prislan, I., and Vesnaver, G., *J. Am. Chem. Soc*., 2012, vol. 134, no. 23, p. 9657.
6. Georgiades, S.N., Abd Karim, N.H., Suntharalingam, K., and Vilar, R., *Angew. Chem. Int. Ed*. 2010, vol. 49, p. 4020.
7. Grand, C.L., Han, H., Munoz, R.M., Weitman, S., Von Hoff, D.D., Hurley, L.H., and Bearss, D.J., *Mol. Cancer Ther*., 2002, vol. 1, no. 8, p. 565.
8. Haider, S.M., Parkinson, G.N., and Neidle, S., *J. Mol. Biol*., 2003, vol. 326, no. 1, p. 117.
9. Chen, B., Liang, J., Tian, X., and Liu, X., *Biochemistry (Moscow),* 2008, vol. 73, p. 853.
10. Wei, C., Wang, J., and Zhang, M., *Biophys. Chem*., 2010, vol. 148, no. 1, p. 51
11. Scatchard, G., *Ann. N.Y. Acad. Sci*., 1949, vol. 51, p. 660.
12. McGhee, J.D. and von Hippel, P.H., *J. Mol. Biol*., 1974, vol. 86, no. 2, p. 469.
13. Crothers, D.M., *Biopolymers,* 1968, vol. 6, no. 4, p. 575.
14. Schwarz, G., *Eur. J. Biochem*., 1970, vol. 12, no. 3, p. 442.
15. Zasedatelev, A.S., Gurskii, G.V., and Vol'kenshtein, M.V., *Mol. Biol*., 1971, vol. 5, no. 2, p. 245.
16. Hill, T.L., *Cooperativity Theory in Biochemistry. Steady State and Equilibrium Systems*, New York: Springer, 1985.
17. Cera, E., *Thermodynamic Theory of Site-Specific Binding Processes in Biological Macromolecules*, Cambridge: Cambridge Univ. Press, 1995.
18. Kudrev, A.G., *Talanta*, 2008, vol. 75, no. 2, p. 380.
19. Kudrev, A.G., *Talanta*, 2012, vol. 101, p. 157.
20. Timoshkin A.Yu. and Kudrev, A.G., *Russ. J. Inorg. Chem*., 2012, vol. 57, no. 10, p. 1362.

21. Kudrev, A.G., *Polym. Sci. Ser. A*, 2000, vol. 42, no. 5, p. 527.
22. Kudrev, A.G., *Russ. J. Gen. Chem*., 2002, vol. 72, no. 10, p. 1501.
23. Kudrev, A.G., *Russ. J. Gen. Chem*., 2006, vol. 76, no. 11, p. 1782.
24. Gargallo, R., Eritja, R., and Kudrev, A.G., *Russ. J. Gen. Chem*., 2010, vol. 80, no. 3, p. 485.
25. Bucek, P., Gargallo, R., and Kudrev, A., *Anal. Chim. Acta*, 2010, vol. 683, no. 1, p. 69.
26. Kudrev, A.G. , *Biophys.*, 2012, vol. 57, no. 3, p. 305.
27. Kudrev, A.G., *Talanta*, 2013, vol. 116, p. 541.
28. Golub, G.H. and Van Loan, C.F., *Matrix Computations*, London: The Johns Hopkins Univ. Press, 1989.
29. Marquardt, D.W., *J. Soc. Ind. Appl. Math*., 1963, vol. 2, no. 2, p. 431.
30. Maeder, M. and Zuberbuhler, A.D., *Anal. Chem*., 1990, vol. 62, p. 2220.
31. Hartley, F. R., Burgess, C., and Alcock, R.M., *Solution Equilibria*, Chichester: Horwood, 1983.
32. Hamilton, W.C., *Statistics in Physical Science*, New York: Roland, 1964.
33. Jaumot, J., Eritja, R., and Gargallo, R., *Anal. Bioanal. Chem*., 2011, vol. 399, p. 1983.
34. Manaye, S., Eritja, R,, Avino, A., Jaumot, J., and Gargallo, R., *Biochim. Biophys. Acta*, 2012, vol. 1820, p. 1987.